Review Article **Open Access**

Lucia Caspani*, Christian Reimer, Michael Kues, Piotr Roztocki, Matteo Clerici, Benjamin Wetzel, Yoann Jestin, Marcello Ferrera, Marco Peccianti, Alessia Pasquazi, Luca Razzari, Brent E. Little, Sai T. Chu, David J. Moss, and Roberto Morandotti*

Multifrequency sources of quantum correlated photon pairs on-chip: a path toward integrated Quantum Frequency Combs

DOI: 10.1515/nanoph-2016-0029
Received October 29, 2015; accepted February 23, 2016

***Corresponding Author: Lucia Caspani:** Institut National de la Recherche Scientifique - Énergie Matériaux et Télécommunications, Université du Québec, 1650 Boulevard Lionel-Boulet, Varennes, Québec, Canada J3X 1S2
and Institute of Photonics and Quantum Sciences, Heriot-Watt University, Edinburgh EH14 4AS, UK, E-mail: lucia.caspani@gmail.com
***Corresponding Author: Roberto Morandotti:** Institut National de la Recherche Scientifique - Énergie Matériaux et Télécommunications, Université du Québec, 1650 Boulevard Lionel-Boulet, Varennes, Québec, Canada J3X 1S2
and Institute of Fundamental and Frontier Sciences, University of Electronic Science and Technology of China, Chengdu 610054, China, E-mail: morandotti@emt.inrs.ca
Christian Reimer, Michael Kues, Piotr Roztocki, Yoann Jestin, Luca Razzari: Institut National de la Recherche Scientifique - Énergie Matériaux et Télécommunications, Université du Québec, 1650 Boulevard Lionel-Boulet, Varennes, Québec, Canada J3X 1S2
Matteo Clerici: Institut National de la Recherche Scientifique - Énergie Matériaux et Télécommunications, Université du Québec, 1650 Boulevard Lionel-Boulet, Varennes, Québec, Canada J3X 1S2
and School of Engineering, University of Glasgow, Glasgow G12 8LT, UK
Benjamin Wetzel, Marco Peccianti, Alessia Pasquazi: Institut National de la Recherche Scientifique - Énergie Matériaux et Télécommunications, Université du Québec, 1650 Boulevard Lionel-Boulet, Varennes, Québec, Canada J3X 1S2
and Department of Physics and Astronomy, University of Sussex, Falmer, Brighton BN1 9RH, UK
Marcello Ferrera: Institut National de la Recherche Scientifique - Énergie Matériaux et Télécommunications, Université du Québec, 1650 Boulevard Lionel-Boulet, Varennes, Québec, Canada J3X 1S2
and Institute of Photonics and Quantum Sciences, Heriot-Watt University, Edinburgh EH14 4AS, UK
Brent E. Little: State Key Laboratory of Transient Optics and Photonics, Xi'an Institute of Optics and Precision Mechanics, Chinese Academy of Science, Xi'an, China
Sai T. Chu: Department of Physics and Materials Science, City University of Hong Kong, Tat Chee Avenue, Hong Kong, China
David J. Moss: Centre for Microphotonics, Swinburne University of Technology, Hawthorn, VIC 3122, Australia

Abstract: Recent developments in quantum photonics have initiated the process of bringing photonic-quantum-based systems out-of-the-lab and into real-world applications. As an example, devices to enable the exchange of a cryptographic key secured by the laws of quantum mechanics are already commercially available. In order to further boost this process, the next step is to transfer the results achieved by means of bulky and expensive setups into miniaturized and affordable devices. Integrated quantum photonics is exactly addressing this issue. In this paper, we briefly review the most recent advancements in the generation of quantum states of light on-chip. In particular, we focus on optical microcavities, as they can offer a solution to the problem of low efficiency that is characteristic of the materials typically used in integrated platforms. In addition, we show that specifically designed microcavities can also offer further advantages, such as compatibility with telecom standards (for exploiting existing fibre networks) and quantum memories (necessary to extend the communication distance), as well as giving a longitudinal multimode character for larger information transfer and processing. This last property (i.e., the increased dimensionality of the photon quantum state) is achieved through the ability to generate multiple photon pairs on a frequency comb, corresponding to the microcavity resonances. Further achievements include the possibility of fully exploiting the polarization degree of freedom, even for integrated devices. These results pave the way for the generation of integrated quantum frequency combs that, in turn, may find important applications toward the realization of a compact quantum-computing platform.

1 Introduction

Quantum photonics is playing an increasingly important role in today's research community, and some applications have already reached the commercial stage. Indeed, one of the preferred carriers for quantum information pro-

cessing, and for communications in particular, is the photon, i.e., the quantum of light. This is mainly due to an intrinsically low decoherence that allows to preserve the photon's quantum state for long time, and thus for long propagation distances.

The main building blocks of quantum information, especially for computing and communications, are entangled photons (pairs of photons that share a single and not separable wave function) and single photons (nonclassical states of the electromagnetic field composed by one and only one photon). The most exploited method for generating these states is spontaneous parametric down conversion (SPDC) in second-order nonlinear crystals [1–5]. In this process, a photon from an excitation field (the only input) is annihilated within the nonlinear crystal and two daughter twin photons (called signal and idler) are generated (Fig. 1A). One of the main advantages of SPDC is its versatility, as it can be exploited for generating either entangled photons in different degrees of freedom (e.g., polarization, position, orbital angular momentum, and more) or heralded single photons. In this last case, the relevant property of the two photons is that they are generated exactly at the same time, and thus can be exploited for heralding the presence of one single photon on the idler beam upon detection of a photon in the signal beam.

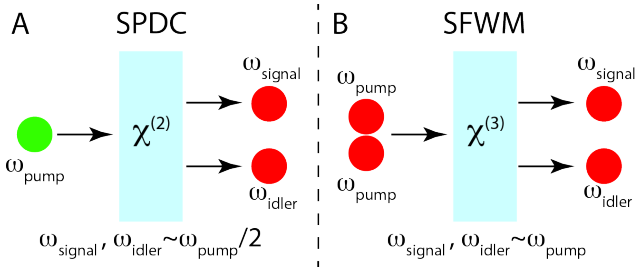

Fig. 1. Spontaneous processes for the generation of (entangled) photon pairs in second-order (A) and third-order (B) nonlinear media, where one or two photons of the pump field are annihilated, respectively, leading to the generation of two daughter photons.

While SPDC is nowadays a common tool in many quantum optical labs for generating quantum states of light, it typically relies on bulky setups and large efforts have been dedicated in the past years for reducing the footprint of these systems [6–8]. Following a trend typical for classical optics, the first step has been the generation of quantum states in optical fibers. Squeezing, quantum correlations, and entangled photon pair generation in different variables have all been achieved in fibers and we refer the reader to the thorough overview on this topic reported in [9]. More recently, with the development of integrated optics, it became clear that the potential of quantum optics may be fully harnessed only in conjunction with the development of an appropriate integrated platform [10]. On the one hand, photonic chips able to realize the logic ports required for quantum computing have been recently demonstrated [11, 12]. On the other hand, an intense research activity has been dedicated to implement on chip sources of single and entangled photons [6, 7, 13–17]. A detailed review on the genesis and evolution of integrated quantum optics can be found in [18].

For practical and ultimately widespread implementation, on-chip devices compatible with electronic integrated circuit technology offer great advantages in terms of low cost, small footprint, high performances and low energy consumption [19]. Furthermore, it is possible to manufacture a large number of such devices on a single chip, in a fully scalable platform. These devices can then be used individually or even combined into complex ensembles. The output of the chip devices can then be fiber coupled to allow easy read-out and further manipulation, as well as compatibility with existing telecommunications infrastructures. However, the materials used in silicon on-chip technology usually feature only a third-order nonlinearity. In $\chi^{(3)}$ media photon pair generation is achieved through spontaneous four-wave mixing (SFWM), where two photons of the excitation field are annihilated, leading to the generation of two daughter photons (Fig. 1B). While there is no fundamental restriction to use third-order nonlinear devices, they typically suffer from different drawbacks such as lower nonlinear coefficients. As mentioned before, one solution was offered by optical fibres, where the low nonlinearity is compensated by the long interaction distance allowed by the mode confinement. Alternatively, a stronger interaction can be achieved exploiting resonant effects because of the field enhancement that they provide. In particular, triply resonant $\chi^{(3)}$ cavities (i.e., cavities where all the three involved fields – pump, signal and idler – are simultaneously resonant) provide a pair production rate improvement that scales as the sixth power of the cavity enhancement factor [20]. For this purpose, slow-light photonic crystal waveguides [21] or microcavities [22] offer the possibility to combine the small footprint with a reasonably high generation rate. Furthermore, exploiting optical cavities for the generation of photon pairs allows one to reduce the photon pair bandwidth [23, 24], eventually matching the bandwidth required by quantum memories without the need of narrowband filters, which are known to reduce the pair production rate.

The compatibility with quantum memories is fundamental in order to allow long-distance quantum key distribution (QKD). Indeed, the fibre losses limit the maxi-

mum distance achievable to a few hundred kilometres. Standard amplifiers cannot be exploited to boost the propagation distance, since this will inevitably compromise the protocol security (this is the essence of single photon based QKD protocols). A possible solution relies on quantum repeaters, i.e., repeater stations in which the signal is not amplified but rather the entanglement of a photon pair over a distance L is achieved by proper combination of two entangled pairs, each extending over a distance $L/2$ [25]. However, a necessary requirement for quantum repeaters is the possibility to store the quantum state of the photon. Since quantum memories are typically based on atomic transitions that have linewidths on the order of 10 to 100 MHz [25], the photon pairs must also exhibit these bandwidths. Many of the sources based on integrated resonators have so far failed to achieve the narrow linewidths compatible with quantum memories because of their relatively modest Q-factors [14, 16, 26–29]. On the other hand, narrow linewidth sources can be achieved by exploiting extremely high Q-factor cavities, however these are fundamentally incompatible with large-scale integration [6, 15, 31–33].

Another important feature allowed by the use of optical cavities for the generation of quantum states is the possibility to achieve multimode entanglement. One of the most exploited degrees of freedom for photon entanglement is polarization – a two-dimensional variable – and therefore the quantum state of the photon is described by a two-dimensional quantum system or qubit (quantum bit). However, for variables with a dimensionality higher than 2 (multimode configuration), the photon state is described by a D-dimensional quantum system, thus passing from qubits to qu$D$its. The higher dimensionality allows one, e.g., to increase the quantity of information carried by a single photon. Different high dimensional variables, either discrete such as orbital angular momentum [34, 35], or continuous such as time (or its conjugate, frequency) [36, 37] and space (or its conjugate, the transverse wave vector) [38] have been considered and investigated in the framework of bulk optics, yet mainly with $\chi^{(2)}$ media.

On the contrary, almost all third-order devices developed so far are limited to the generation of two-mode single correlated states, and multiple correlated photon generation has only recently been investigated on chip [27, 39, 40]. In the next section, we report on our efforts toward the first realization of a wavelength-multiplexed source of heralded single photons on a chip compatible with both quantum memories and electronic chip fabrication processes (CMOS, complementary metal-oxide semiconductor compatibility) [39]. We defined the obtained state as a "quantum frequency comb," to mean that we generate quantum states (in this case heralded single photons) distributed on a frequency comb. This broad definition encompasses other quantum frequency combs in literature (see, for example, the discussion in Section 4. *Conclusions and Outlook*), where quantum correlations (e.g., squeezing) between the frequency modes allow for further applications of quantum frequency combs.

2 Frequency comb of correlated photon pairs and heralded single photons: wavelength multiplexing

The requirements of a scalable and commercializable source for practical use include long-term operational stability and insensitivity to environmental changes, compatibility with quantum memories, operation at telecomm wavelengths (near 1550 nm), and the possibility of using large-scale electronic chip fabrication processes (CMOS). The development of such a source thus faces significant challenges, since quantum memories are typically associated with high-Q resonators, but external pumping of these cavities leads to meta-stable pump configurations due to thermal and environmental changes. While it is possible to lock an external excitation field to a single resonator, for example, by using active electronic locking, not only does this dramatically increase the complexity of the system, rendering it incompatible with full integration on a chip, but it can actually lead to very unstable operation.

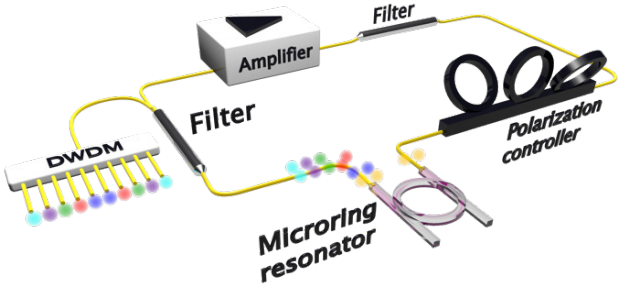

Fig. 2. Experimental setup for the generation of multiplexed photon pairs in the self-locked pumping scheme: the pump photons (yellow) are filtered and redirected to the amplifier for sustaining the pump lasing, while correlated photon pairs are demultiplexed by means of a dense wavelength division multiplexing (DWDM) filter before detection.

In order to solve the critical and difficult issue of locking the excitation field to the ring resonances, we have developed a novel pumping scheme relying on passive optical feedback in a nested cavity-pumping configuration. By embedding the microring resonator in an external active cavity, locking is directly achieved within the pump laser. Lasing is self-started by the amplified spontaneous emission of the active gain medium employed (fibre amplifier) and is then sustained by reinjecting a single ring resonance (the pump field, selected by a tunable narrowband filter) into the amplifier (see Fig. 2).

A frequency comb of photons is generated through SFWM, excited by this stable pump configuration, where two ν_0 excitation photons are annihilated and two photons at $\nu_0 + n\Delta\nu$ and ν_0-$n\Delta\nu$, respectively, are generated. In this case, ν_0 is the pump frequency, $\Delta\nu$ is the microring free spectral range (FSR, 200 GHz in our case), and n is an integer. Since the signal/idler photons are generated in a single quantum process, their temporal correlation is expected to give a peak at zero delay. This peak is broadened, however, by the fact that, once generated, the photons can exit the cavity at different times, following the characteristic lifetime of the cavity, determined by the ring resonator linewidth. In particular, for typical Lorentzian resonances, it is thus expected a signal-idler temporal correlation of the form $C_{si}(\tau) \propto \exp(-2\pi\delta\nu|\tau|)$, where $\delta\nu$ is the cavity linewidth and τ is the signal-idler delay [23]. The correlation function is typically measured by detecting signal and idler photons with single photon detectors that are able to discriminate their arrival time with a resolution better than the cavity lifetime, thus providing the coincidence rate as a function of the signal-idler delay.

In order to achieve CW (continuous wave) oscillation, which is preferable for generating high-coherence photon pairs, the FSR of the external cavity has to be large enough, and ideally larger than the microring linewidth ($\delta\nu$ =140 MHz in our case), so that only a single line of the external cavity oscillates [41]. Note that a long pump coherence time corresponds to a large alphabet (the dimensionality is essentially given by the ratio between the pump coherence time and the photon pair bandwidth, in turn determined by the cavity lifetime), i.e., high number of bits of information per photon [37]. When using an amplifier with a long gain medium (e.g., a standard erbium-doped fiber amplifier, EDFA), the external cavity length is typically of the order of tens of meters, leading to a FSR well below the ring resonance linewidth. This, in turn, leads to the oscillation of many lines (e.g., 24 for a 30 m long fibre amplifier) of the external cavity, resulting in chaotic lasing [42]. In addition, this chaotic pump behavior leads to the formation of isolated high peak-power pulses, which significantly lowers the threshold for optical parametric oscillation (OPO). Indeed, low-threshold OPO in this pump configuration was demonstrated at an average input power of only 6 mW [42]. In the unstable pump configuration, pulses oscillate inside the pump cavity with a repetition rate defined by the FSR of the external cavity (6 MHz, see Fig. 3A). These high-power peaks lead to the generation of multiple photon pairs per pulse (even at very low average pump powers), that can lead to a spread of the coincidence peak. This happens, for example, when the detected signal and idler photons do not belong to a single pair, but are generated in different down conversion events, separated in time.

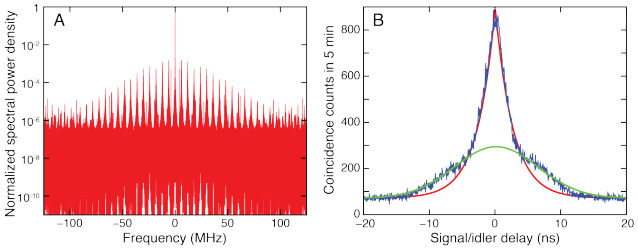

Fig. 3. A. Radiofrequency spectrum of the unstable pump configuration, showing a clear pulsed operation with 6 MHz repetition rate. B. Coincidence peak measured in the unstable pump configuration (blue curve). A superposition of two peaks is visible, where the narrow signal/idler peak (fitted by the C_{si} function, in red) is superimposed with a larger peak (fitted by a Gaussian function, in green).

This, in turn, can be seen in the coincidence measurement, where this effect manifests in the superposition of a narrow and a wide peak (see Fig. 3B). The narrow peak corresponds to the real signal/idler coincidences, while the wide peak is caused by coincidences between uncorrelated photon pairs generated within the same pulse.

In order to enable CW oscillation even with a long external cavity, we have inserted a narrowband Fabry–Perot filter selecting only one external cavity line (see detailed experimental setup in Fig. 4). In this case a CW oscillation can be achieved, as shown in the measured radiofrequency (RF) spectrum (Fig. 5A). With a CW pump, only a narrow coincidence peak is visible as shown in Fig. 5B, underlining that the issue of multi-photon generation is eliminated in the stable CW pump configuration. It is worth noting that the issue of stability associated to the locking between the external pump laser and the ring resonances, is much more relevant for the high Q-factor microcavities that are needed to achieve high generation efficiencies while matching the narrow linewidths required for atomic-based quantum memories. For very high Q-factor

ring resonators, such as the one employed in this work, the locking between the external CW laser and the resonance is usually lost after a few minutes, especially at the low pump powers typically used for photon pair generation. In our configuration instead, any thermal fluctuation is passively locked and the pump scheme allows for long-term stability, with no need for external, active feedback. One of the most promising features of the scheme that we developed is its potential to be fully monolithically integrated, enabling the practical implementation of microresonator-based quantum light sources. By using our novel self-locked excitation scheme, we demonstrated an integrated photon pair source that generates multiple, simultaneous, and independent photon pairs multiplexed and distributed on a frequency comb grid that is compatible with the ITU (International Telegraph Union) channel spacing of optical fibre communications networks. In fact, although we limited our investigation to five channel pairs, our device is capable of generating photon pairs on a comb over a bandwidth that exceeds the telecom C and L bands (1530 to 1620 nm), corresponding to more than 80 different signal/idler channel pairs. The source is extremely stable, operating continuously for several weeks with less than 5% fluctuation in photon flux, without any active stabilization.

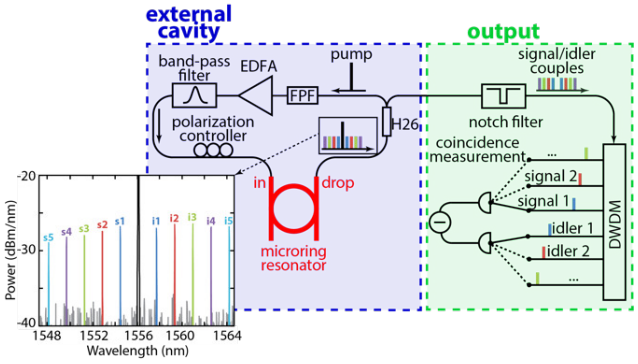

Fig. 4. Detailed experimental setup showing the Fabry-Pérot filter (FPF) used to select a single external cavity resonance for achieving true CW pumping. The inset shows the spectrum of the generated photons (the black line is the pump). Adapted from Ref. [39].

Using an integrated high-Q (1.375 million) microring resonator, we were able to achieve the generation of heralded single photons on five independent channels (centered at standard telecom channels, separated by 200 GHz).

Measurements of the signal-idler correlation function for all the pair configurations of the first five resonances around the excitation frequency demonstrate the correlated photon pair emission only on resonance pairs spectrally symmetric to the pump frequency (Fig. 6). For each channel pair, we obtained coincidence to accidental ratios (CARs) between 10 and 14, coincidence rates between 26.4 and 48.4 Hz (without background subtraction), and single rates between 8.5 and 10 kHz. Taking into account detector dark counts, the losses of the detection system (losses after the microring and detector quantum efficiency) and a nearly constant rate for the ~80 channels, we find a total pair production rate on all the channels of ~25 MHz, a value higher or comparable to most of the experiments based on integrated silicon microrings. On the other hand, the CAR obtained is still modest, but different strategies such as reducing the losses by integrating more components on the same chip or the use of better detectors can be employed to improve it. Finally, we estimated a heralding efficiency, i.e., the probability of detecting an idler photon upon detection of the signal one, of ~10% [39].

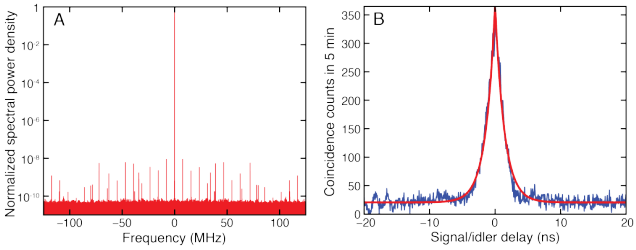

Fig. 5. A. RF spectrum of the pump configuration with the long EDFA and narrowband Fabry-Pérot filter showing clear CW operation. The noise at non-zero frequencies is caused by the limited dynamic range of the oscilloscope. B. Coincidence peak measured in the CW pump configuration using the long EDFA with the FP filter (blue curve), together with the corresponding C_{si} fit (red curve).

The source also features linewidths (110 MHz) that are orders of magnitude narrower than previous sources based on integrated ring resonators, and that are thus compatible with atomic-based quantum memories.

We note that a fundamental feature for applications in quantum cryptography is indeed the generation of heralded single photons. In particular, quantum states of light composed of one photon are the main component of QKD systems, based for example on the BB84 protocol [43]. In this protocol, the cryptographic key is encoded in the quantum state of a single photon and security is provided by (i) the fact that a single photon is the ultimate quantum of the radiation and cannot be partially detected to gain information on its state; (ii) the impossibility to clone an unknown quantum state (no-cloning theorem [44, 45]); (iii) the impossibility to measure a quantum state without perturbing it (and thus without being detected). As mentioned in the introduction, photon pair sources based on nonlin-

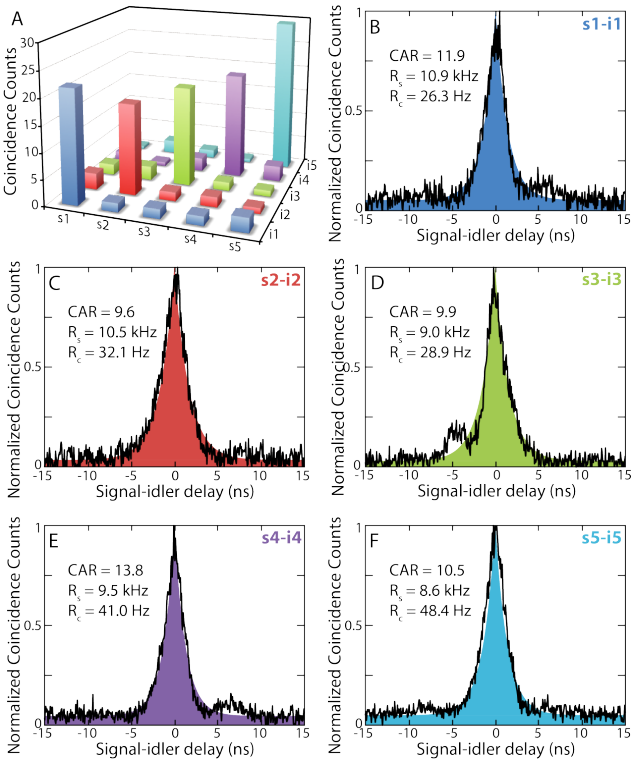

Fig. 6. A. Coincidence count rate measured at all the signal/idler combinations. Significant coincidence counts (corresponding to a peak) are only visible between symmetric channels. B-F Normalized coincidence peaks (corrected for the dark counts due to the detector noise) measured for the 5 symmetric channel pairs (black curves) with the relative Csi fit (solid-shaded curves). In each panel the measured CAR, single rate (Rs) and coincidence rate (Rc) are reported.

ear processes (either $\chi^{(2)}$ or $\chi^{(3)}$), can be used as single photon sources exploiting the fact that the twin photons are emitted simultaneously. Therefore, in order to actually demonstrate a heralded single photon source we need to prove that upon detection of a photon in, for example, the signal arm, we have one photon in the idler arm. This can be done inserting a beam splitter on the idler arm and measuring the coincidence between its output ports when a single photon has been detected on the signal arm. For a true twin photon source, only a single photon is present in the idler arm, and therefore no coincidences are expected after the beam splitter (see Fig. 7A). More precisely, a heralded single photon source is demonstrated when the heralded idler–idler correlation $g_h^{(2)}$ shows a dip at zero delay lower than 0.5. We perform this measurement with our setup and found that $g_h^{(2)}$ =0.144<0.5 (Fig. 7B).

Finally, the device is based on a platform that is compatible with electronic computer chip technology. All together, these features potentially mark a substantial step forward to achieve stable, integrated, and CMOS-

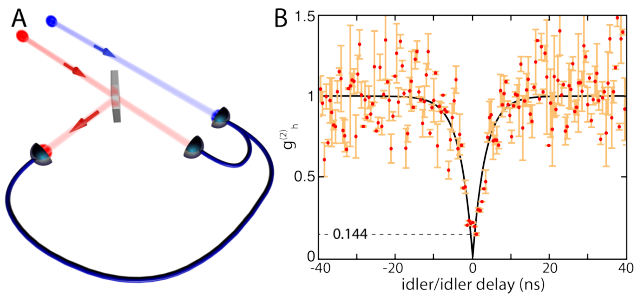

Fig. 7. A. Scheme for heralded $g^{(2)}$ measurement. The signal photon (blue) is detected and triggers the other two detectors. The idler photon (red) can exit one or the other beam splitter ports (the lower one in the picture), but not both. This results in a dip in the coincidence measurement heralded by the detection of a signal photon (B). Figure partially adapted from [39].

compatible multimode sources for quantum optical applications. While in this particular case only heralded single photons were generated, it has been shown that, for example, energy-time or time-bin entanglement can be generated using SFWM on chip [28, 29]. In particular, by combining time-bin entanglement and the wavelength multiplexing approach, we recently demonstrated the generation of bi- and multiphoton-entangled qubits [30].

3 Cross-polarized photon pair generation

As discussed in Section 2, entanglement generation using second-order nonlinear interactions made use of, in certain implementations, polarization as an important degree of freedom to entangle photons between different modes. In this section, we review our recent demonstration of frequency mixing between orthogonal polarization modes in a compact integrated microring resonator and the demonstration of a bichromatically pumped optical parametric oscillator [46]. In addition, we contextualize this result in the framework of quantum frequency comb generation.

Most applications exploiting nonlinear processes in either bulk media or fiber-based devices have extensively relied on the electric field polarization as a fundamental degree of freedom to achieve novel nonlinear functionalities. In particular, different configurations can be exploited for parametric processes depending on the relative polarization of the pump(s) and generated fields: Type-0 (the pump and generated fields are copolarized); Type-I (the generated fields are copolarized but different from the pump polarization); and Type-II (the generated fields have orthogonal polarizations). However, in-

tegrated third-order devices have not been able to exploit all of these degrees of freedom. While several on-chip key components have been developed, to date polarization has not been fully exploited as a degree of freedom for the realization of novel integrated nonlinear devices. In particular, frequency conversion based on orthogonally polarized beams has not yet been demonstrated on chip. Multipolarization processes, e.g., nondegenerate type-II spontaneous FWM where the two excitation photons come from two distinct polarization fields, could, in principle, be achieved on-chip by using two orthogonally polarized pump fields, similarly to the fiber case [47, 48]. However, the overlapping and dominant stimulated processes generally make spontaneous FWM experimentally undetectable. Furthermore, to achieve efficient frequency conversion in a small footprint, integrated nonlinear processes are often enhanced through the use of cavities or photonic crystal waveguides, but these structures are typically designed for single polarization operation, as most integrated waveguides show a strong polarization-dependent dispersion and loss. Achieving efficient Type-II spontaneous FWM on a chip therefore requires structures that not only operate on two orthogonal polarizations with specific dispersion properties, but also provide nonlinear enhancement while suppressing competing stimulated processes.

It is important to stress that, with respect to previous results in which polarization-entangled photons have been achieved on-chip (see, e.g., [17]), we exploit here a novel nonlinear process never observed so far in integrated structures. For example, in Ref. [17], the authors combined two different generation processes to achieve polarization entanglement. In particular, their structure is designed to obtain Type-0 SFWM on TE modes in the first half waveguide and Type-0 SFWM on TM modes in the second half. By properly engineering the pump polarization, this can result in polarization-entangled photon pairs. This remarkable result follows the lead of polarization entanglement in bulk $\chi^{(2)}$ materials obtained by combining two type-I BBO crystals with different orientations [49]. While this is a valid alternative to directly using a type-II process, the latter continues to be the most exploited means of generating polarization-entangled photons. Future developments in this research direction will focus on the demonstration of entanglement.

Furthermore and in what follows, we exploit a slightly modified version of the pump configuration presented in Section 2, since the self-locked scheme also enables the stable excitation of two or more pump ring lines at the same time. By exciting two resonances of orthogonal polarization modes, we introduced a new type of spontaneous four-wave mixing to the toolbox of integrated photonics. In particular, we demonstrated the first realization of Type-II spontaneous FWM. This scheme allows, for the first time, the direct generation of orthogonally-polarized photon pairs on a chip.

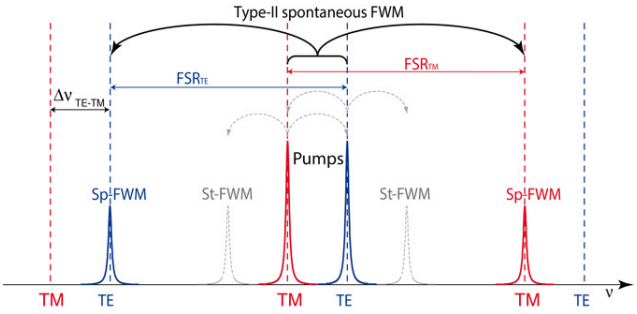

Fig. 8. Scheme of the relations required between TE and TM FSRs in order to suppress stimulated FWM between the two cross-polarized pump fields. Figure from [46].

In order to demonstrate this novel configuration, we used a microring resonator operating on the fundamental transverse electric (TE) and transverse magnetic (TM) modes, both having similar yet slightly different dispersions. Cavity enhancement is provided by the high Q-factors of the TE and TM resonances (235,000 and 470,000, respectively), which readily enable high parametric gain at low pump powers. In our scheme, the suppression of stimulated FWM between the two excitation fields was obtained by generating a frequency offset of 70 GHz between the TE and TM resonances, while keeping the free spectral ranges of both modes almost identical (200.39 and 200.51 GHz in this experiment), thus allowing Type-II spontaneous FWM to take place at targeted resonances without the presence of stimulated FWM. This offset is generated by the slightly different dispersions of the TE and TM modes, resulting in different effective resonator lengths and hence different resonant frequencies. Energy conservation dictates that the stimulated FWM bands have to be symmetric with respect to the two pump frequencies. Due to the frequency offset between the TE and TM resonances, the spectral position of the stimulated FWM gain does not overlap with the ring resonances, thus suppressing this process inside the microring resonator (Fig. 8). At the same time, the TE and TM mode dispersions have to be kept similar so that the difference in FSR between the two modes (120 MHz) is smaller than the bandwidth of the resonances, in order to achieve energy conservation for Type-II spontaneous FWM processes. Finally, the required

phase-matching condition can be obtained by operating in a slightly anomalous dispersion regime for both modes.

We note that in general the cross-polarized process is nine times less efficient than the copolarized case in which all the fields have the same polarization [46]. In addition, we have to take into account the different Q-factors of the TE and TM resonances. Indeed, the pair production rate scales as $Q_{Pump1} \cdot Q_{Pump2} \cdot Q_{Signal} \cdot Q_{Idler}$ corresponding to Q_{TE}^4 or Q_{TM}^4 in the copolarized case and to $Q_{TE}^2 \cdot Q_{TM}^2$ in our cross-polarized case. This means that in our case where Q_{TM} =2Q_{TE} the copolarized TM case is the most efficient, the copolarized TE case is 16 times less efficient, and the cross-polarized case is as much as 36 times less efficient. Nevertheless, we did observe the generation of cross-polarized photon pairs and obtained heralded single photons.

As discussed earlier, in order to simultaneously pump two resonances, we used a hybrid self-locked pumping approach, where the laser pumping the TE mode was directly built around the resonator, thus eliminating the need for active stabilization (Fig. 9). The microring resonator was embedded inside an external cavity that included a fiber amplifier and a wavelength filter. The amplified spontaneous emission of the fibre amplifier was transmitted through a band-pass filter (100 GHz) centered at the desired TE ring resonance and was then injected into the chip. Light coupled out of the drop port of the ring resonator was fed back to the amplifier, thereby closing the external pump cavity and promoting lasing on the TE mode. In order to allow self-locked lasing on the TE polarization only, while pumping the TM mode with an external laser (actively locked to the resonance using a feedback loop), polarizing beam couplers were placed before and after the ring resonator. This hybrid approach based on the use of one self-locked and one external excitation field permits pumping on both resonances in a very stable configuration and provides precise control over the individual pump powers.

When operated below the OPO threshold, our device directly generated orthogonally polarized photon pairs. In order to characterize them and confirm the nature of the underlying nonlinear process, we performed photon coincidence measurements. The photon pairs generated in the TE and TM modes of the microring resonator were collected at the ring through port after appropriate filtering of both pump fields by means of a polarization-maintaining, high-isolation 200 GHz wide notch filter. The generated photons were then separated by a polarizing beam splitter and detected with single-photon detectors. We measured a clear coincidence peak with a coincidence-to-accidental

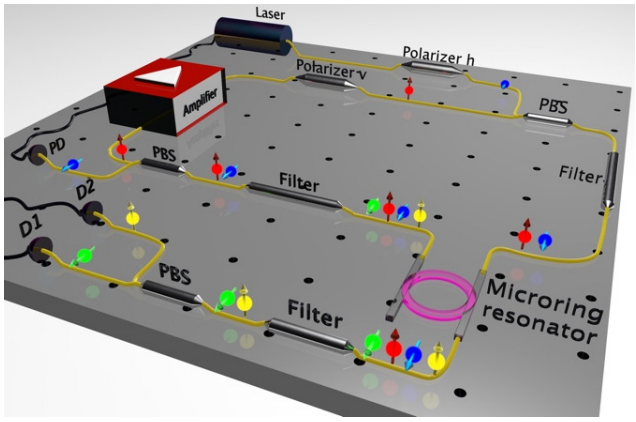

Fig. 9. Experimental setup for achieving spontaneous four wave mixing between two cross-polarized pump fields. The scheme presented in previous section has been improved to allow pumping on two ring resonances. Figure from [46].

ratio (CAR) of up to 12 without any background subtraction (Fig. 10A).

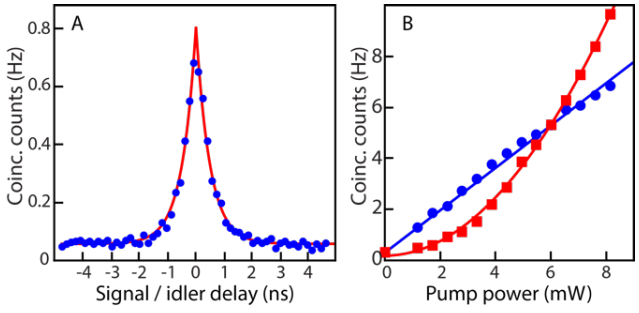

Fig. 10. A. Coincidence peak of the cross-polarized photon pairs (blue points). The red curve is the C_{si} fit. B. Coincidence count scaling as a function of the pump powers for balanced pumps (red squares, with quadratic fit – red curve) and when the power of one pump is kept constant at 6 mW (blue circles, with linear fit – blue curve). Figure adapted from [46].

As photon pairs can only be generated via spontaneous nonlinear processes, the measured photon coincidences give a strong indication that the photon pairs are generated through Type-II spontaneous FWM, with stimulated processes being successfully suppressed. The power-scaling behavior provides further insight into the process associated with the generation of the photon pairs. Only when one photon from each pump field is used to create two daughter photons, it becomes possible to directly generate orthogonally polarized photon pairs. Therefore, the coincidence counts (CC) are expected to scale with the product of both pump powers (CC $\propto$ $P_{TE} \times P_{TM}$). If the power of one pump field is kept constant, and the power of the second one is increased, a linear scaling behav-

ior is predicted for Type-II spontaneous FWM, whereas if the power of both pump fields is simultaneously increased (with constant power ratio), a quadratic scaling is expected instead. No coincidences (within the noise) were measured when the ring was not pumped or pumped with the TE field alone, where the nonzero counts are due to the dark counts of the detector. A clear linear scaling behavior is visible (Fig. 10B) with increasing TM pump power and constant TE power, while a quadratic (without linear contribution) scaling is observed with increasing balanced pump powers. The presence of Raman scattering can be neglected, as the signal and idler frequencies do not overlap significantly with the Raman gain spectrum. This is also experimentally confirmed by the absence of any linear contribution to the power scaling that would arise from any Raman scattering (Fig. 10B).

From the coincidence measurement, shown in Fig. 10A, we extract a measured photon bandwidth of 320 MHz (red curve), which is in good agreement with the resonator bandwidth of 410 MHz associated with the particular ring resonator used in this experiment, where the difference can be explained by the timing jitter of the detectors and electronics that results in a small temporal broadening of the measured peak. It is worth noting that the narrow linewidth, required for several quantum applications, is intrinsically achieved inside the resonator and cannot be directly realized in nonresonant waveguides or fiber-based architectures. The measured CAR of up to 12 is limited by loss, dark counts and the quantum efficiency of the detectors as well as by the photons generated through type-0 SFWM of the individual pumps. These are issues that can be easily addressed in the future by optimizing the device dispersion. We measure a coincidence rate of around 4 Hz at 5 mW balanced pump power at the input of the chip (5mW is the highest achievable pump power featured by a CAR above 10). Considering all losses of the detection system (8.5 dB for both signal and idler) as well as the quantum efficiency of the detectors (5% and 10%, respectively), this corresponds to a pair production rate of 40 kHz and a pair production probability of 1.48×10^{-12}, accounting for the 1.6 dB coupling loss of the pump into the chip. By using better detectors and eventually implementing low-loss filtering on chip, the measured coincidence rate can be further increased to approach the production rate. Finally, also for this cross-polarized case, we performed a heralded $g^{(2)}$ measurement. The measured dip $g_h^{(2)}(0)=0.26 < 0.5$ demonstrate the single photon character of the heralded source (Fig. 11).

The generation of cross-polarized photon pairs is not limited to only the adjacent resonances, but frequency-multiplexed cross-polarized photon pairs are also possible. Indeed, we measured cross-polarized photon pairs over 12 resonance pairs (limited by the available filters) each with pair production rates above 20 kHz at 5 mW balanced pump power. Therefore, also in this case, we can achieve a quantum frequency comb, or more precisely two frequency combs, either with TE modes on the longer wavelengths and TM on the shorter wavelengths, or vice versa.

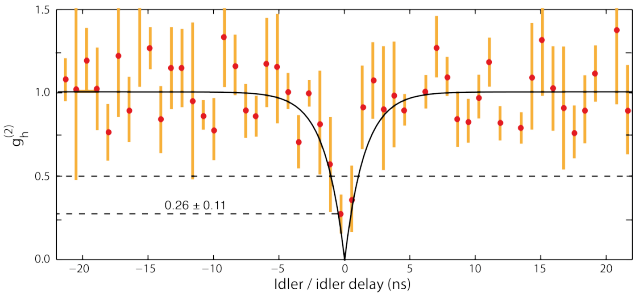

Fig. 11. . Heralded $g^{(2)}$ measurement for the cross-polarized case. Figure adapted from [46].

It is also worth noting that, by further increasing the pump powers it is also possible to achieve above threshold optical parametric oscillation, where relatively intense cross-polarized signal and idler fields can be generated.

Having achieved Type-II spontaneous FWM in an integrated platform, we provide additional access to polarization as a degree of freedom for integrated third-order spontaneous nonlinear interactions. Furthermore, with our scheme two different FWM processes become accessible on the same chip. This opens up the possibility of using, for example, type-0 and type-II FWM simultaneously to generate complex quantum optical states (e.g., multi-entangled states spanning both wavelength and polarization) on a compact platform. All of these characteristics highlight the significant potential of our device for quantum optical applications.

4 Conclusions and Outlook

With integrated quantum photonics reaching a high level of maturity, novel systems able to generate increasingly complex quantum states, with respect to the standard two-photon entangled qubits, can now be envisioned in an integrated platform. For example, entanglement between two identical integrated sources has been demonstrated, which opens up the possibility to implement multiple sources and entangle them to form a larger state [50].

Furthermore, we believe that the future of integrated quantum optics should take advantage of the decennial know-how developed in the framework of bulk quantum optics, and capitalize on the most recent achievements, rather than reproducing its historical development in an integrated fashion. To this purpose, one of the path that is emerging as very promising, also in light of the foreseen and desirable application of quantum technologies out-of-the-lab, relies on multimode quantum states. While these have been widely investigated, they still represent a niche with respect to the more common two-dimensional states based on photon polarization. On the one hand, multimode states represent a valid solution for increasing the amount of information carried by a single photon, thus directly addressing the issue of a low bit rate in the exchange of a quantum cryptographic key. On the other hand, they have been investigated as a possible platform for quantum computing. Indeed, a particular class of multimode quantum states, known as cluster states [51], in which each mode is entangled with more than one of the other modes, has been recently proposed as a novel approach to quantum computing, exploiting the so called one-way quantum computing [51–53]. In the standard circuit quantum computing model, one requires to implement evolution and control on each individual qubit [54]: the quantum algorithms are performed through the different transformations (logic gates) applied to the qubits. This, in turn, strongly hinders the scalability of such systems. We note, however, that in the one-way quantum computing the complexity is shifted from the state control and manipulation to its generation: the different algorithms are realized simply through different measurements. In particular, recent developments in bulk optics [55–60], indicate that quantum frequency combs may represent a viable solution for one-way quantum computing. In light of this, our recent results on the generation of wavelength multiplexed photon pairs in microring resonators demonstrate that this is a venue that should be investigated in integrated platforms. In addition, the possibility to use polarization as degree of freedom for microring-based parametric processes adds a further control tool for achieving this goal.

Acknowledgment: This work was supported by the Natural Sciences and Engineering Research Council of Canada (NSERC) through the Steacie and Discovery Grants Schemes, and by the Australian Research Council (ARC) Discovery Projects program. C.R. and P.R. acknowledge the support of an NSERC Vanier Canada Graduate Scholarship and NSERC Alexander Graham Bell Canada Graduate Scholarship-Master's (CGS-M), respectively. M.K. acknowledges support from FRQNT (Fonds de Recherche du Québec–Nature et Technologies) through the Merit Scholarship Program for Foreign Students; Ministère de l'Éducation, de l'Enseignement Supérieur et de la Recherche du Québec. We acknowledge the support from the People Programme (Marie Curie Actions) of the European Union's FP7 Programme: L.C. for THREEPLE under REA grant agreement n° [627478], B.W. for INCIPIT under REA grant agreement n° [625466], M.C. for KOHERENT under REA grant agreement n° [299522], M.F. for ATOMIC under REA grant agreement n° [329346], M.P. for THEIA under REA grant agreement n° [630833], and A.P. for CHRONOS under REA grant agreement n° [327627]. S.T.C. acknowledges the support from the CityU SRG-Fd program #7004189.

References

[1] W. H. Louisell, A. Yariv, and A. E. Siegman, "Quantum fluctuations and noise in parametric processes. I.," Phys. Rev. **124**, 1646–1654 (1961).

[2] D. N. Klyshko, "Coherent photon decay in a nonlinear medium," Pis'ma Zh. Eksp. Teor. Fiz. **6**, 490 (1967).

[3] S. A. Akhmanov, V. V. Fadeev, R. V. Khokhlov, and O. N. Chunaev, "Quantum noise in parametric light amplifers," Pis'ma Zh. Eksp. Teor. Fiz. **6**, 575–578 (1967).

[4] S. E. Harris, M. K. Oshman, and R. L. Byer, "Observation of tunable optical parametric fluorescence," Phys. Rev. Lett. **18**, 732–734 (1967).

[5] D. Magde and H. Mahr, "Study in ammonium dihydrogen phosphate of spontaneous parametric interaction tunable from 4400 to 16 000 Å," Phys. Rev. Lett. **18**, 905–907 (1967).

[6] E. Pomarico, B. Sanguinetti, N. Gisin, R. Thew, H. Zbinden, G. Schreiber, A. Thomas, and W. Sohler, "Waveguide-based OPO source of entangled photon pairs," New J. Phys. **11**, 113042 (2009).

[7] R. Horn, P. Abolghasem, B. J. Bijlani, D. Kang, A. S. Helmy, and G. Weihs, "Monolithic source of photon pairs," Phys. Rev. Lett. **108**, 153605 (2012).

[8] K.-H. Luo, H. Herrmann, S. Krapick, B. Brecht, R. Ricken, V. Quiring, H. Suche, W. Sohler, and C. Silberhorn, "Direct generation of genuine single-longitudinal-mode narrowband photon pairs," New J. Phys. **17**, 73039 (2015).

[9] G. Agrawal, *Applications of Nonlinear Fiber Optics*, 2nd ed. (Academic Press, 2008).

[10] J. O'Brien, B. Patton, M. Sasaki, and J. Vučković, "Focus on integrated quantum optics," New J. Phys. **15**, 035016 (2013).

[11] A. Politi, M. J. Cryan, J. G. Rarity, S. Yu, and J. L. O'Brien, "Silica-on-silicon waveguide quantum circuits," Science **320**, 646–649 (2008).

[12] A. Politi, J. C. F. Matthews, and J. L. O'Brien, "Shor's quantum factoring algorithm on a photonic chip," Science **325**, 1221 (2009).

[13] H. Takesue, Y. Tokura, H. Fukuda, T. Tsuchizawa, T. Watanabe, K. Yamada, and S. Itabashi, "Entanglement generation using silicon wire waveguide," Appl. Phys. Lett. **91**, 201108 (2007).

[14] S. Clemmen, K. Phan Huy, W. Bogaerts, R. G. Baets, P. Emplit, and S. Massar, "Continuous wave photon pair generation in silicon-on-insulator waveguides and ring resonators," Opt. Express **17**, 16558–16570 (2009).
[15] J. U. Fürst, D. V. Strekalov, D. Elser, A. Aiello, U. L. Andersen, C. Marquardt, and G. Leuchs, "Quantum light from a whispering-gallery-mode disk resonator," Phys. Rev. Lett. **106**, 113901 (2011).
[16] S. Azzini, D. Grassani, M. J. Strain, M. Sorel, L. G. Helt, J. E. Sipe, M. Liscidini, M. Galli, and D. Bajoni, "Ultra-low power generation of twin photons in a compact silicon ring resonator," Opt. Express **20**, 23100–23107 (2012).
[17] N. Matsuda, H. Le Jeannic, H. Fukuda, T. Tsuchizawa, W. J. Munro, K. Shimizu, K. Yamada, Y. Tokura, and H. Takesue, "A monolithically integrated polarization entangled photon pair source on a silicon chip," Sci. Rep. **2**, 817 (2012).
[18] S. Tanzilli, A. Martin, F. Kaiser, M. P. De Micheli, O. Alibart, and D. B. Ostrowsky, "On the genesis and evolution of integrated quantum optics," Laser Photon. Rev. **6**, 115–143 (2012).
[19] D. J. Moss, R. Morandotti, A. L. Gaeta, and M. Lipson, "New CMOS-compatible platforms based on silicon nitride and Hydex for nonlinear optics," Nature Phot. **7**, 597–607 (2013).
[20] L. G. Helt, Z. Yang, M. Liscidini, and J. E. Sipe, "Spontaneous four-wave mixing in microring resonators," Opt. Lett. **35**, 3006 (2010).
[21] M. J. Collins, M. J. Steel, T. F. Krauss, B. J. Eggleton, and A. S. Clark, "Photonic crystal waveguide sources of photons for quantum communication applications," IEEE J. Sel. Top. Quantum Electron. **21**, 205–214 (2015).
[22] K. J. Vahala, "Optical microcavities," Nature **424**, 839–846 (2003).
[23] Z. Ou and Y. Lu, "Cavity enhanced spontaneous parametric down-conversion for the prolongation of correlation time between conjugate photons," Phys. Rev. Lett. **83**, 2556–2559 (1999).
[24] K. Garay-Palmett, Y. Jeronimo-Moreno, and a B. U'Ren, "Theory of cavity-enhanced spontaneous four wave mixing," Laser Phys. **23**, 015201 (2013).
[25] N. Sangouard, C. Simon, H. de Riedmatten, and N. Gisin, "Quantum repeaters based on atomic ensembles and linear optics," Rev. Mod. Phys. **83**, 33–80 (2011).
[26] E. Engin, D. Bonneau, C. M. Natarajan, A. S. Clark, M. G. Tanner, R. H. Hadfield, S. N. Dorenbos, V. Zwiller, K. Ohira, N. Suzuki, H. Yoshida, N. Iizuka, M. Ezaki, J. L. O'Brien, and M. G. Thompson, "Photon pair generation in a silicon micro-ring resonator with reverse bias enhancement," Opt. Express **21**, 27826–27834 (2013).
[27] R. Kumar, J. R. Ong, J. Recchio, K. Srinivasan, and S. Mookherjea, "Spectrally multiplexed and tunable-wavelength photon pairs at 1.55 μm from a silicon coupled-resonator optical waveguide," Opt. Lett. **38**, 2969–2971 (2013).
[28] D. Grassani, S. Azzini, M. Liscidini, M. Galli, M. J. Strain, M. Sorel, J. E. Sipe, and D. Bajoni, "Micrometer-scale integrated silicon source of time-energy entangled photons," Optica **2**, 88 (2015).
[29] C. Xiong, X. Zhang, A. Mahendra, J. He, D.-Y. Choi, C. J. Chae, D. Marpaung, A. Leinse, R. G. Heideman, M. Hoekman, C. G. H. Roeloffzen, R. M. Oldenbeuving, P. W. L. van Dijk, C. Taddei, P. H. W. Leong, and B. J. Eggleton, "Compact and reconfigurable silicon nitride time-bin entanglement circuit," Optica **2**, 724 (2015).
[30] I. C. Reimer, M. Kues, P. Roztocki, B. Wetzel, F. Grazioso, B. E. Little, S. T. Chu, T. Johnston, Y. Bromberg, L. Caspani, D. J. Moss, and R. Morandotti, "Generation of multiphoton entangled quantum states by means of integrated frequency combs," Science **351**, 1176–1180 (2016).
[31] M. Förtsch, J. U. Fürst, C. Wittmann, D. Strekalov, A. Aiello, M. V Chekhova, C. Silberhorn, G. Leuchs, and C. Marquardt, "A versatile source of single photons for quantum information processing," Nat. Commun. **4**, 1818 (2013).
[32] C.-S. Chuu, G. Y. Yin, and S. E. Harris, "A miniature ultrabright source of temporally long, narrowband biphotons," Appl. Phys. Lett. **101**, 051108 (2012).
[33] F. Monteiro, a. Martin, B. Sanguinetti, H. Zbinden, and R. T. Thew, "Narrowband photon pair source for quantum networks," Opt. Express **22**, 4371 (2014).
[34] J. Leach, B. Jack, J. Romero, A. K. Jha, A. M. Yao, S. Franke-Arnold, D. G. Ireland, R. W. Boyd, S. M. Barnett, and M. J. Padgett, "Quantum correlations in optical angle-orbital angular momentum variables," Science **329**, 662–665 (2010).
[35] A. C. Dada, J. Leach, G. S. Buller, M. J. Padgett, and E. Andersson, "Experimental high-dimensional two-photon entanglement and violations of generalized Bell inequalities," Nature Phys. **7**, 677–680 (2011).
[36] I. Ali Khan and J. Howell, "Experimental demonstration of high two-photon time-energy entanglement," Phys. Rev. A **73**, 031801 (2006).
[37] I. Ali-Khan, C. Broadbent, and J. Howell, "Large-alphabet quantum key distribution using energy-time entangled bipartite states," Phys. Rev. Lett. **98**, 060503 (2007).
[38] M. Kolobov, "The spatial behavior of nonclassical light," Rev. Mod. Phys. **71**, 1539–1589 (1999).
[39] C. Reimer, L. Caspani, M. Clerici, M. Ferrera, M. Kues, M. Peccianti, A. Pasquazi, L. Razzari, B. E. Little, S. T. Chu, D. J. Moss, and R. Morandotti, "Integrated frequency comb source of heralded single photons," Opt. Express **22**, 6535–6546 (2014).
[40] W. C. Jiang, X. Lu, J. Zhang, O. Painter, and Q. Lin, "Silicon-chip source of bright photon pairs," Opt. Express **23**, 20884 (2015).
[41] M. Peccianti, A. Pasquazi, Y. Park, B. E. Little, S. T. Chu, D. J. Moss, and R. Morandotti, "Demonstration of a stable ultrafast laser based on a nonlinear microcavity," Nat. Commun. **3**, 765 (2012).
[42] A. Pasquazi, L. Caspani, M. Peccianti, M. Clerici, M. Ferrera, L. Razzari, D. Duchesne, B. E. Little, S. T. Chu, D. J. Moss, and R. Morandotti, "Self-locked optical parametric oscillation in a CMOS compatible microring resonator: a route to robust optical frequency comb generation on a chip," Opt. Express **21**, 13333 (2013).
[43] C. H. Bennett and G. Brassard, "Quantum cryptography: public key distribution and coin tossing," in *IEEE International Conference on Computers, Systems and Signal Processing* (1984), pp. 175–179.
[44] W. K. Wootters and W. H. Zurek, "A single quantum cannot be cloned," Nature **299**, 802–803 (1982).
[45] D. Dieks, "Communication by EPR devices," Phys. Lett. A **92**, 271–272 (1982).
[46] C. Reimer, M. Kues, L. Caspani, B. Wetzel, P. Roztocki, M. Clerici, Y. Jestin, M. Ferrera, M. Peccianti, A. Pasquazi, B. E. Little, S. T. Chu, D. J. Moss, and R. Morandotti, "Cross-polarized

photon-pair generation and bi-chromatically pumped optical parametric oscillation on a chip," Nat. Commun. **6**, 8236 (2015).

[47] Q. Lin, F. Yaman, and G. Agrawal, "Photon-pair generation in optical fibers through four-wave mixing: Role of Raman scattering and pump polarization," Phys. Rev. A **75**, 023803 (2007).

[48] E. Brainis, "Four-photon scattering in birefringent fibers," Phys. Rev. A **79**, 023840 (2009).

[49] P. G. Kwiat, E. Waks, A. G. White, I. Appelbaum, and P. H. Eberhard, "Ultrabright source of polarization-entangled photons," Phys. Rev. A **60**, R773–R776 (1999).

[50] J. W. Silverstone, R. Santagati, D. Bonneau, M. J. Strain, M. Sorel, J. L. O'Brien, and M. G. Thompson, "Qubit entanglement between ring-resonator photon-pair sources on a silicon chip," Nat. Commun. **6**, 7948 (2015).

[51] R. Raussendorf and H. J. Briegel, "A one-way quantum computer," Phys. Rev. Lett. **86**, 5188–5191 (2001).

[52] N. C. Menicucci, P. van Loock, M. Gu, C. Weedbrook, T. C. Ralph, and M. a. Nielsen, "Universal quantum computation with continuous-variable cluster states," Phys. Rev. Lett. **97**, 110501 (2006).

[53] J. Zhang and S. L. Braunstein, "Continuous-variable Gaussian analog of cluster states," Phys. Rev. A **73**, 032318 (2006).

[54] M. A. Nielsen and I. L. Chuang, *Quantum Computation and Quantum Information* (Cambridge University Press, 2000).

[55] S. Yokoyama, R. Ukai, S. C. Armstrong, C. Sornphiphatphong, T. Kaji, S. Suzuki, J. Yoshikawa, H. Yonezawa, N. C. Menicucci, and A. Furusawa, "Ultra-large-scale continuous-variable cluster states multiplexed in the time domain," Nature Phot. **7**, 982–986 (2013).

[56] O. Pfister, S. Feng, G. Jennings, R. Pooser, and D. Xie, "Multipartite continuous-variable entanglement from concurrent nonlinearities," Phys. Rev. A **70**, 020302 (2004).

[57] O. Pinel, P. Jian, R. M. de Araújo, J. Feng, B. Chalopin, C. Fabre, and N. Treps, "Generation and characterization of multimode quantum frequency combs," Phys. Rev. Lett. **108**, 083601 (2012).

[58] J. Roslund, R. M. de Araújo, S. Jiang, C. Fabre, and N. Treps, "Wavelength-multiplexed quantum networks with ultrafast frequency combs," Nature Phot. **8**, 109–112 (2013).

[59] M. Pysher, Y. Miwa, R. Shahrokhshahi, R. Bloomer, and O. Pfister, "Parallel generation of quadripartite cluster entanglement in the optical frequency comb," Phys. Rev. Lett. **107**, 030505 (2011).

[60] M. Chen, N. C. Menicucci, and O. Pfister, "Experimental realization of multipartite entanglement of 60 modes of a quantum optical frequency comb," Phys. Rev. Lett. **112**, 120505 (2014).